Talanta 115 (2013) 577–582

Contents lists available at SciVerse ScienceDirect

Talanta

journal homepage: www.elsevier.com/locate/talanta

Amplified electrochemiluminescence of luminol based on hybridization chain reaction and in situ generate co-reactant for highly sensitive immunoassay

Lijuan Xiao, Yaqin Chai *, Ruo Yuan *, Yaling Cao, Haijun Wang, Lijuan Bai

Education Ministry Key Laboratory on Luminescence and Real-Time Analysis, College of Chemistry and Chemical Engineering, Chongqing 400715, People's Republic of China

ARTICLE INFO

Article history:
Received 10 April 2013
Received in revised form
7 June 2013
Accepted 16 June 2013
Available online 21 June 2013

Keywords:
Electrochemiluminescence
Luminol
Hybridization chain reaction
Glucose oxidase
Hydrogen peroxide
Immunosensor

ABSTRACT

In this work, we described a simple and highly sensitive electrochemiluminescence (ECL) strategy for IgG detection. Firstly, L-cysteine functionalized reduced graphene oxide composite (L-cys-rGO) was decorated on the glassy carbon electrode (GCE) surface. Then anti-IgG was immobilized on the modified electrode surface through the interaction between the carboxylic groups of the L-cys-rGO and the amine groups in anti-IgG. And then biotinylated anti-IgG (bio-anti-IgG) was assembled onto the electrode surface based on the sandwich-type immunoreactions. By the conjunction of biotin and streptavidin (SA), SA was immobilized, which in turn, combined with the biotin labeled initiator strand (S1). In the presence of two single DNA strands of glucose oxidase labeled S2 (GOD-S2) and complementary strand (S3), S1 could trigger the hybridization chain reaction (HCR) among S1, GOD-S2 and S3. Herein, due to HCR, numerous GOD was efficiently immobilizated on the sensing surface and exhibited excellent catalysis towards glucose to in situ generate amounts of hydrogen peroxide (H_2O_2), which acted as luminol's co-reactant to significantly enhance the ECL signal. The proposed ECL immunosensor presented predominate stability and high sensibility for determination of IgG in the range from 0.1 pg mL^{-1} to 100 ng mL^{-1} with a detection limit of 33 fg mL^{-1} ($S/N=3$). Additionally, the designed ECL immunosensor exhibited a promising application for other protein detection.

1. Introduction

Electrochemiluminescence (ECL), involving a light emission process in a redox reaction of electrogenerated reactants at electrode surface, combines the controllability of electrochemistry with the sensitivity of luminescent techniques and shows high selectivity, reproducibility, low background and wide dynamic concentration response range [1,2]. By integrating ECL technology with immunoassay, the ECL-based immunosensors have attracted intensive and extensive research interests due to its rapidity, simplicity, flexibility and easy controllability [3,4]. Up to now, a series of light-emitting systems using co-reactant for signal amplification have been applied in ECL immunosensors including luminol-H_2O_2 [5,6], $Ru(bpy)_3^{2+}$-tripropylamine [7,8], $S_2O_8^{2-}$–O_2 [9,10] and semiconductor nanocrystals-$S_2O_8^{2-}$ systems [11,12]. Among them, luminol-H_2O_2 system has been widely used due to its high emission yields, low oxidation potential and inexpensive reagent consumption. However, as the most widely used co-reactant of luminol, H_2O_2 has the disadvantages of instability in the detection solution and difficulty to label. Researchers found that in situ generating H_2O_2 was a fascinating method to overcome the above shortages. In our previous work, we proposed a high sensitivity ECL immunosensor by coupling enzymatic reaction of GOD to in situ generate H_2O_2 with Au or Pd nanoparticles as catalyst for the ECL reaction [13,14]. It is worth to be mentioned that the loading amount of GOD has an important influence on the ECL signal of luminol. Thus, it is necessary to explore effective methods to improve the immobilization of GOD and further enhance the sensitivity of luminol-H_2O_2 system.

Recently, the employment of DNA as amplified indicators attracts great attention [15–17]. DNA-based amplification techniques mainly including hybridization chain reaction (HCR), ligase chain reaction (LCR), polymerase chain reaction (PCR) and rolling circle amplification (RCA) [18–21]. Among these amplification methods, HCR is an especially promising isothermal approach for signal enhancement. HCR is triggered by an initiator strand and leads to a long nicked double helices analogous (dsDNA). Since it is an initiator triggered enzyme-free reaction, it produces a comparable reduced background signals and an impressive detection limits. Besides, the HCR can be operated at mild conditions. Based

* Corresponding authors. Tel.: +86 23 68252277; fax: +86 23 68253172.
E-mail addresses: yqchai@swu.edu.cn (Y. Chai), yuanruo@swu.edu.cn (R. Yuan).

0039-9140/$ - see front matter © 2013 Elsevier B.V. All rights reserved.
http://dx.doi.org/10.1016/j.talanta.2013.06.027

on HCR signal amplification, great improvements on the performances of the biosensor are realized. For instance, Zhao et al. [22] reported an electrochemical aptasensor for interferon-gamma detection based on the HCR with enzyme-signal amplification. Our group also reported a highly sensitive strategy for ECL detection of DNA sequence based on HCR. The signal amplification relied on the HCR-induced formation of dsDNA polymers on the sensing surface and the intercalation of massive ECL indicators into the dsDNA grooves [23]. Inspired by the excellent amplification capability of HCR, we reported a new ECL immunosensor based on the HCR to enhance the immobilization of GOD to in situ generate H_2O_2 as co-reactant of luminol.

Furthermore, biocompatible L-cysteine (L-cys) is widely used in biosensors for the reason that it has many functional groups for biomolecular binding [24,25]. And it has been reported that L-cys has a great enhancement to the ECL intensity of luminol [26]. Conseding its functional groups, L-cys was used in our work to connect reduced graphene oxide (rGO) through its $-NH_2$ groups and antibodies through its –COOH groups. Graphene oxide (GO) is an excellent platform for biosensor construction due to its unique electronic, thermal and mechanical properties [27–30]. The excellent biocompatibility and large surface area of graphene oxide (GO) allows it to be an efficient carrier to load more active probes and active domains [4]. Considering the above mentioned factors, L-cys-rGO nanocomposites were synthesized in our work, which act as a sensor platform not only facilitated the electron transfer but also presented an abundant domain for biomolecular binding and further improved the performances of the immunosensor.

Herein, we present a new strategy to construct an ECL immunosensor for sensitive detection of IgG based on HCR to improve the immobilization of GOD and enzymatic reaction of GOD to in situ generate H_2O_2 as luminol's co-reactant. Due to the advantages of high specific surface and enhanced electron transport properties, L-cys-rGO was used as a sensor platform to immobilize anti-IgG. In the presence of target IgG, the sandwiched antigen–antibody immunocomplex could be formed between the immobilized anti-IgG and the biotinylated anti-IgG (bio-anti-IgG). Using the binding of biotin–streptavidin conjugates, SA was assembled on the electrode surface, which in turn combined with the biotin labeled initiator strand (S1). Then, S1 triggered the hybridization chain reaction (HCR) between glucose oxidase labeled S2 (GOD-S2) and complementary strand (S3). Thus multiple GOD was efficiently attached on the sensing surface through HCR and exhibited excellent catalysis towards glucose to in situ generate amounts of H_2O_2. Coupling HCR with in situ co-reactant, the proposed ECL immunosensor exhibited sensitive and stable response for detection of IgG and showed great potential in clinical applications.

2. Experimental section

2.1. Materials and reagents

Graphene oxide (GO) was purchased from Nanjing xianfeng nano Co. (Nanjing, China). Poly(ethylenimine) (PEI, 50%) was obtained from Fluka (Switzerland). The L-cysteine (L-cys) was purchased from Kangan Amino Acid Company (Shanghai, China). Glutaraldehyde (GA), glucose oxidase (GOD), bovine serum albumin (BSA, 96–99%), luminol (98%) were purchased from Sigma-Aldrich Chem. Co. (St. Louis, MO, USA). Goat anti-mouse IgG (anti-IgG), mouse IgG, biotinylated goat anti-mouse IgG (bio-anti-IgG) and streptavidin (SA) were obtained from Beijing Biosynthesis Biotechnology Co. Ltd. (Beijing, China). N-hydroxysuccinimide (NHS) and N-(3-dimethylaminopropyl)-N-ethylcarbodiimidehydrochloride (EDC) were purchased from Shanghai Medpep Co. Ltd. (Shanghai, China). Labeled oligonucleotides were synthesized by Takara Biotechnology Co. Ltd. (Dalian, China). The sequences of these oligomers were:

S1: 5′-boi-CGGCACCTGGGGGAGTATTGCGGAGGAAGGTGCCG-3′
S2: 5′-CGGCACCTGGGGGAGTATTGCGGAGGAAGGTGCCG–NH_2-3′
S3: 5′-TACTCCCCCAGGTGCCGACGGCACCTTCCTCCGCA-3′

Phosphate buffered solution (PBS) (pH 7.4, 0.1 M) containing 0.1 M Na_2HPO_4, 0.1 M KH_2PO_4 and 0.1 M KCl was used to prepare antigen, antibody and SA solutions. Ferricyanide/ferrocyanide mixed solution ($[Fe(CN)_6]^{3-/4-}$, 5.0 mM, pH 7.4) were obtained by dissolving potassium ferricyanide and potassium ferrocyanide with PBS (pH 7.4). Tris–HCl buffer (pH 7.4, 0.1 M) with 500 mM NaCl and 1 mM $MgCl_2$ was used to prepare enzyme solutions and used as hybridization buffer. The standard stock solutions were prepared with PBS (pH 7.4) and stored at 4 °C before use. All reagents were used as received without further purification and double-distilled water was used throughout this study.

2.2. Apparatus and measurements

The ECL emission was monitored by a model MPI-A electrochemiluminescence analyzer (Xi' an Remax Electronic Science & Technology Co. Ltd., Xi' an, China). All experiments were performed with a three-electrode setup, which contained a platinum wire as counter electrode, an Ag/AgCl (sat. KCl) as reference electrode and a prepared glassy carbon electrode (Φ=4 mm) as working electrode. The voltage of the photomultiplier tube (PMT) was maintained at 800 V and the applied potential was 0.2–0.8 V (vs. Ag/AgCl) with a scan rate of 100 mV s^{-1}. Cyclic voltammetric (CV) measurements were taken with a CHI 600B electrochemistry workstation (Shanghai CH Instruments, China). X-ray photoelectron spectroscopy (XPS) measurements were performed with a VG Scientific ESCALAB 250 spectrometer, using Al Ka X-ray (1486.6 eV) as the light source.

2.3. Preparation of the L-cys-rGO nanocomposites

The schematic diagram of the stepwise process for synthesizing L-cys-rGO was shown in Fig. S1 (see the supplementary material). Firstly, using PEI as reductants, the reduced graphene oxide (rGO) was prepared according to the literature with a little modification [31–33]. Briefly, a stable dispersion of exfoliated GO sheets (17 mL, 1.0 mg mL^{-1}) was mixed with PEI (1.5 mL, 3%) and heated under reflux at 135 °C for 3 h. The rGO was obtained by centrifugation and washed three times with double-distilled water. Here, rGO provided abundant amino for further association of L-cys with the aid of GA. Secondly, GA (0.5 mL, 2.5%) and L-cys (0.02 M, 0.1 M HCl) were added into the prepared rGO solution under gently stirring to produce the L-cys-rGO. Subsequently, free GA and L-cys were removed by centrifugation and the resulting precipitates were washed with double-distilled water at least three times. Then the target product was dispersed in double-distilled water and stored at 4 °C for further use. The as-prepared L-cys-rGO was characterized by XPS. As shown in Fig. S2 (see the supplementary material), the appearance of N1s and S2p peaks in the XPS survey spectrum indicated the combination of rGO with L-cys.

2.4. Preparation of GOD-S2

Prior to experiment, GOD (50 μL, 1 mg mL^{-1}), GA (60 μL, 2.5%) and S2 (200 μL, 2.5 μM) were added into 1 mL PBS (pH 7.4). Then, the mixture was slightly stirred for about 3 h at 4 °C. During this process, GOD was conjugated to S2 via the covalent binding between the free amino groups at its 3′ terminus and the amino groups of GOD. Then, GOD-S2 was stored in 4 °C when not in use.

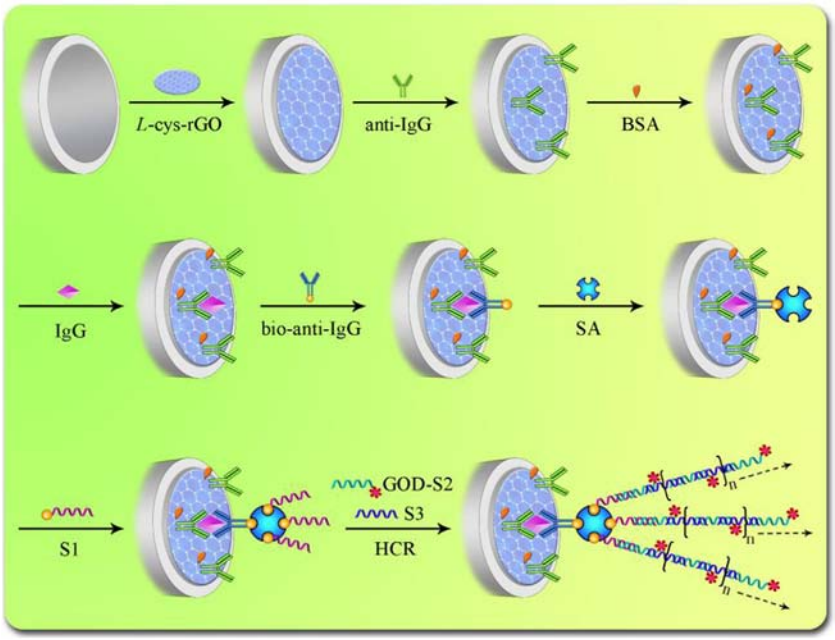

Fig. 1. The fabrication process of the immunosensor.

2.5. Fabrication of the ECL immunosensor

The schematic graph of the fabrication process was depicted in Fig. 1. A glassy carbon electrode (GCE, Φ=4 mm) was successively polished with 0.3 and 0.05 μm alumina slurries and sonicated sequentially in double-distilled water, ethanol and double-distilled water for 5 min. Subsequently, a droplet of 10 μL L-cys-rGO was coated onto the pretreated electrode and allowed to dry in air. The activation solution (100 mM NHS and 400 mM EDC in double-distilled water, 20 μL) was then dipped onto the surfaces to activate the carboxyl groups of L-cys-rGO for 4 h at 4 °C. And then the obtained electrode was immersed into anti-IgG solution (200 μg mL^{-1}) at 4 °C for 10 h. Thus, the antibody molecules were introduced to the electrode via the Schiff-bonds of the interaction between the active carboxylic groups of the L-cys-rGO and the amine groups in anti-IgG. To block the possible remaining active sites, 10 μL of 1% BSA was placed onto the electrode for 1 h. After that, the modified electrode was incubated with various concentrations of IgG for 1 h at 25 °C. After the binding reaction between anti-IgG and IgG, the electrode was immersed into bio-anti-IgG solution (40 ng mL^{-1}) for 1 h. Subsequently, 10 μL SA (2.0 mg mL^{-1}) was placed onto the modified electrode surface and incubated for 30 min. Then, the electrode was incubated with 20 μL S1 solution for 30 min. Following that, a mixture of GOD-S2 and S3 were dipped onto the surfaces for 100 min resulting in the formation of glucose oxidize labeled double-stranded DNA (GOD-dsDNA) molecules. The modified electrode was rinsed thoroughly with PBS (pH 7.4) to remove the nonspecifically bound species after every modificatory step. Thus the proposed electrode was constructed successfully.

3. Results and discussion

3.1. Characterization of the ECL immunosensor

In order to characterize the fabrication process of the ECL immunosensor, ECL signals were recorded after each electrode modification step. As shown in Fig. 2 (A), a very weak ECL signal was observed on the bare GCE (curve a). The ECL signal increased after L-cys-rGO was modified on the bare electrode (curve b), because the L-cys-rGO improved the electron transfer at the electrode interface. However, when anti-IgG was immobilized onto the electrode, the ECL signal decreased greatly (curve c). The reason was that the protein on the electrode hindered the diffusion of luminescent reagents toward the electrode surface. When the antigen molecules reacted with the antibody molecules, a decreased ECL response was obtained (curve d), as the formed antigen–antibody complex had an insulation effect in the ECL reaction. And the ECL intensity further decreased when the bio-anti-IgG was coupled covalently onto the IgG on the modified electrode (curve e), for that the protein hindered the electron transfer. By the special reaction of SA and biotin, SA and S1 were assembled on the electrode surface resulting in a successive decrease of the ECL signal (curves f and g). After the HCR among S1, GOD-S2 and S3, massive GOD molecules were linked to the sensing surface and the ECL signal decreased (curve h). Finally, when 10^{-2} M glucose was added into the detection solution, these attached GOD efficiently catalyzed the glucose to in situ generate amounts of H_2O_2, which largely amplified the ECL signal (curve i).

To gain a better understanding of the fabrication process of the ECL immunosensor, the cyclic voltammograms (CVs) experiments were also performed in 5 mM $[Fe(CN)_6]^{3-/4-}$ solution. As shown in Fig. 2 (B), the L-cys-rGO/GCE (curve b) exhibited higher current than bare GCE (curve a), which was due to the excellent electronic transmission ability of L-cys-rGO. However, when anti-IgG was immobilized on the L-cys-rGO layer modified electrode (curve c), peak current decreased dramatically for the hindrance of non-conductive antibody molecules. After incubating with IgG, the CV responses further declined because the antigen–antibody immunocomplex could obstruct the electron transfer (curve d). And then the peak current decreased clearly when incubated with SA (curve e), for that the protein hindered the electron transfer. When the immunosensor was incubated with S1, a decrease of current was observed (curve f), due to the repulsion of ferricyanide from the electrode surface by the negative charges of the DNA backbones. After the HCR, the CV signal decreased obviously (curve h). It was attributed to the DNA sequences and protein GOD retard the electron transfer tunnel.

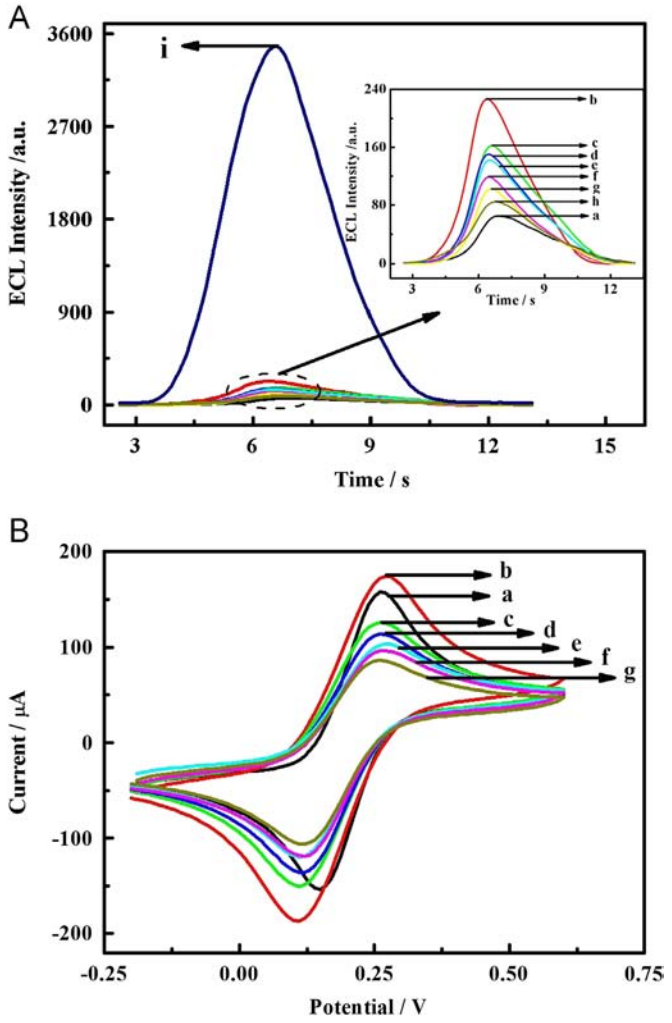

Fig. 2. (A) ECL profiles of (a) bare GCE, (b) L-cys-rGO/GCE, (c) anti-IgG/L-cys-rGO/GCE, (d) IgG/BSA/anti-IgG/L-cys-rGO/GCE, (e) bio-anti-IgG/IgG/BSA/anti-IgG/L-cys-rGO/GCE, (f) SA/bio-anti-IgG/IgG/BSA/anti-IgG/L-cys-rGO/GCE, (g) S1/SA/bio-anti-IgG/IgG/BSA/anti-IgG/L-cys-rGO/GCE, (h) GOD-dsDNA/S1/SA/bio-anti-IgG/ IgG/BSA/anti-IgG/L-cys-rGO/GCE, in 2 mL 0.1 M PBS (pH 7.4) with 10^{-3} M luminol. (i) after the addition of 10^{-2} M glucose in the detection solution. (B) CVs for (a) bare GCE, (b) L-cys-rGO/GCE, (c) anti-IgG/L-cys-rGO/GCE, (d) IgG/BSA/anti-IgG/L-cys-rGO/GCE, (e)SA/bio-anti-IgG/ IgG/BSA/anti-IgG/L-cys-rGO, (f) S1/SA/bio-anti-IgG/IgG/BSA/anti-IgG/L-cys-rGO, (g) GOD-dsDNA/S1/SA/bio-anti-IgG/IgG/ BSA/anti-IgG/L-cys-rGO in 5.0 mM $[Fe(CN)_6]^{3-/4-}$ (pH 7.4) at scan rate of 100 mV s^{-1}.

3.2. Optimization of analytical conditions

The reaction time of the biological recognition pairs (i.e. IgG/anti-IgG and SA/biotin), which has a direct influence on the quantity of protein molecules loaded onto the electrode and thus impact the ECL signals, had been investigated by Mao et al. [34]. To further improve the detection sensitivity, the incubation time of the HCR with 10 ng mL^{-1} IgG was discussed in this paper. As shown in Fig. 3, the ECL signals increased gradually with the augment of incubation time. However, after about 100 min the ECL signals tended to be constant, which indicated that the reaction equilibrium was reached. Thus, 100 min was employed as the optimum time for HCR in this experiment.

3.3. Comparison of different labeled electrodes

After the S1/SA/bio-anti-IgG/IgG/BSA/anti-IgG/L-cys-rGO modified electrode incubating with GOD-S2 molecules for 100 min, a weak ECL signal was obtained when detected in 2 mL PBS (pH 7.4)

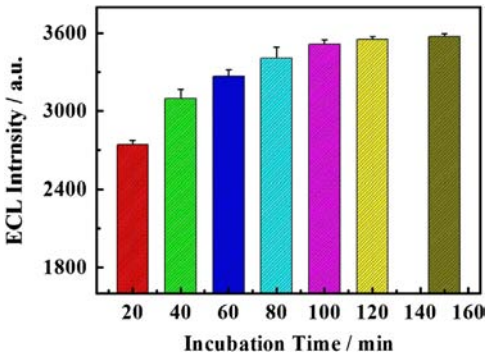

Fig. 3. Effect of the incubation time on HCR amplification with 10 ng mL^{-1} IgG.

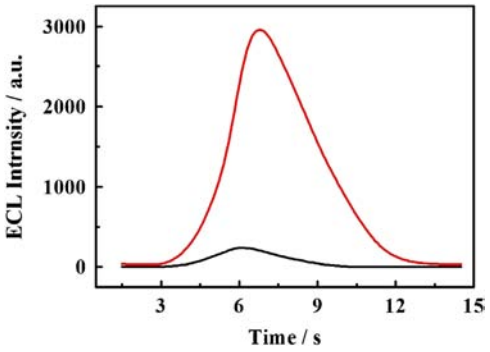

Fig. 4. The ECL response of the GOD-S2/S1/SA/bio-anti-IgG/IgG/BSA/anti-IgG/L-cys-rGO modified GCE (black curve) and GOD-dsDNA/S1/SA/bio-anti-IgG/IgG/BSA/anti-IgG/L-cys-rGO modified GCE (red curve) with 1.0 ng mL^{-1} IgG in 2 mL 0.1 M PBS (pH 7.4) containing 10^{-3} M luminol and 10^{-2} M glucose at scan rate of 100 mV s^{-1}. (For interpretation of the references to color in this figure legend, the reader is referred to the web version of this article).

containing10^{-3} M luminol and 10^{-2} M glucose (black curve in Fig. 4). However, when incubated with the mixture of GOD-S2 and S3, the HCR was happened and led to the formation a long nicked dsDNA molecule containing multiple GOD. These localized GOD exhibited efficient catalysis towards glucose to in situ generate H_2O_2 for luminol ECL, achieving a significant higher ECL signal (red curve in Fig. 4).

3.4. ECL detection of IgG with the immunosensor

To assess the sensitivity and quantitative range of the proposed immunoassay, the immunoassay format was employed to detect different concentrations of IgG. The ECL responses were recorded under continuous scanning to obtain a relative steady ECL signals. Upon increasing the target concentration, the ECL signals increased accordingly (Fig. 5 (insert)). As shown in Fig. 5, the calibration plots displayed a good linear relationship between the ECL signal and the logarithm of IgG concentrations in the range from 0.1 pg mL^{-1} to 100 ng mL^{-1} with a detection limit of 33 fg mL^{-1} ($S/N=3$). The regression equation was $I=2918.36+517.06 \log c_{IgG}$ with a correlation coefficient of 0.9991 (Where I was the ECL intensity (a.u.), and c_{IgG} was the concentration of IgG). The results demonstrated that the proposed immunosensor could be used to detect IgG concentration quantitatively. As shown in Table S1, the proposed immunosensor exhibited wider response range and much higher sensitivity compared with other IgG immunosensors. The reason may be as follows: amounts of GOD were immobilized on the modified electrode surface due to the HCR. This GOD could exhibite excellent catalysis towards glucose to in situ generate amounts of H_2O_2. Then H_2O_2 could enhance the ECL reaction of luminol and then improve the sensitivity of the immunosensor.

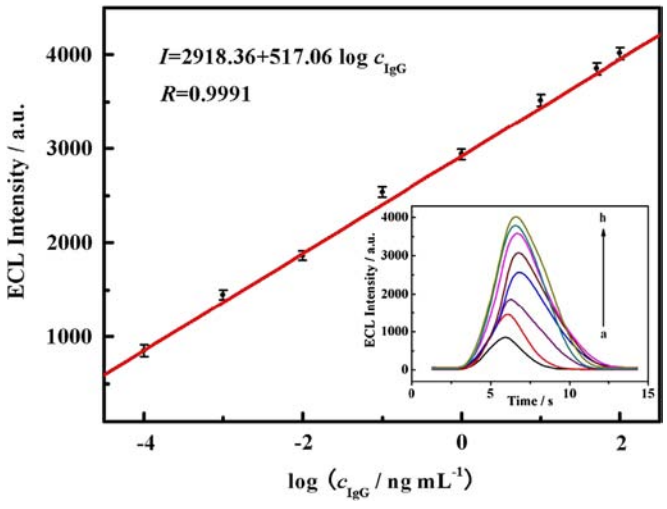

Fig. 5. Calibration curve for IgG assay. Inset: ECL responses of the proposed immunosensor to different concentrations of IgG: (a) 0.1 pg mL^{-1}, (b) 1.0 pg mL^{-1}, (c) 0.01 ng mL^{-1}, (d) 0.1 ng mL^{-1}, (e) 1.0 ng mL^{-1}, (f) 10 ng mL^{-1}, (g) 50 ng mL^{-1} and (h) 100 ng mL^{-1}.

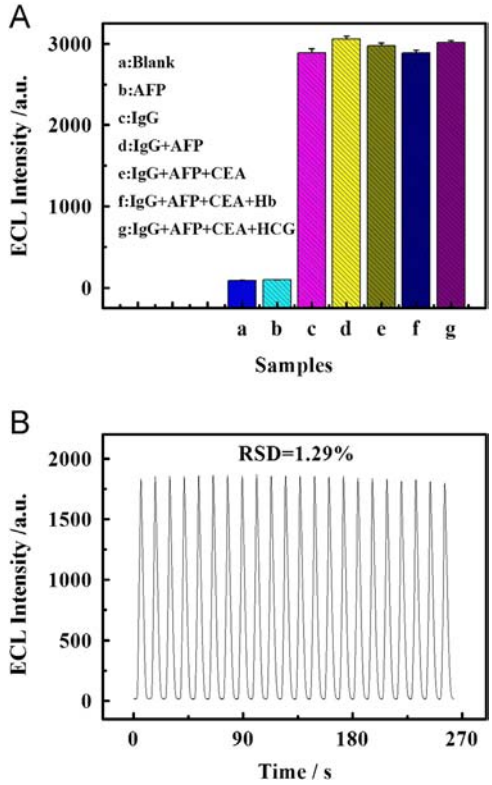

Fig. 6. (A) The selectivity of the proposed ECL immunosensor: (a) blank, (b) AFP (1 ng mL^{-1}), (c) IgG (1 ng mL^{-1}), (d) a mixture containing IgG (1 ng mL^{-1}), AFP (20 ng mL^{-1}), (e) a mixture containing IgG (1 ng mL^{-1}), AFP (20 ng mL^{-1}) and CEA (20 ng mL^{-1}), (f) a mixture containing IgG (1 ng mL^{-1}), AFP (20 ng mL^{-1}), CEA (20 ng mL^{-1}) and Hb (20 ng mL^{-1}), (g) a mixture containing IgG (1 ng mL^{-1}), AFP (20 ng mL^{-1}), CEA (20 ng mL^{-1}) and HCG (20 mIU mL^{-1}). (B) The stability of the proposed ECL immunosensor incubated with 0.01 ng mL^{-1} IgG under consecutive cyclic potential scans. All ECL signals were measured in 2 mL 0.1 M PBS (pH 7.4) containing 10^{-3} M luminol and 10^{-2} M glucose.

3.5. Selectivity, precision, reproducibility and stability

To investigate the selectivity and specificity of the proposed immunosensor, contrast experiments were performed (Fig. 6 (A)).

Table 1
The recovery of the proposed immunosensor in normal human serum.

Sample number	Add/ng mL^{-1}	Found/ng mL^{-1}	Recovery/%
1	0.05	0.055	109.8
2	0.1	0.103	103.1
3	1.0	0.986	98.6
4	10.0	10.06	100.6
5	20.0	21.05	105.3

The immunosensor was incubated with 1 ng mL^{-1} IgG containing different interfering species such as α-fetoprotein (AFP), carcinoembryonic antigen (CEA), hemoglobin (Hb) and human chorionic gonadotrophin (HCG). As shown from Fig. 6 (A), no remarkable signal was observed in comparison with that in the presence of IgG only. The immunosensor was also incubated in 1 ng mL^{-1} AFP, almost no signal change was obtained when compared with the background. These results clearly demonstrated the high selectivity of the proposed immunosensor for IgG.

The precision and reproducibility of the proposed immunosensor were evaluated by the variation coefficients of intra- and inter-assays. The intra-assay precision was 4.86%, which was estimated by testing the 1.0 ng mL^{-1} IgG for replicate measurements with six different electrodes in the same batch. Similarly, the inter-assay precision was 5.23%, which was evaluated from the response to 1.0 ng mL^{-1} IgG with six immunosensors made at the same GCE with various batches. Hence, the precision and reproducibility of the proposed immunosensor were acceptable.

Fig. 6 (B) showed the ECL signal of the immunosensor under consecutive cyclic potential scans for 22 cycles. Stable and high ECL signals were observed. The outstanding stability may be attributed to the following reasons: first, L-cys-rGO provided a good matrix for the loading of antibody, which could increase the access chance of the antigen and GOD-dsDNA molecules. Second, due to HCR was operated at mild conditions, the loaded GOD kept its good bioactivity and exhibited excellent catalysis towards glucose to in situ generate amounts of H_2O_2. Third, the co-reactant, H_2O_2, produced in situ, was more stable and efficient to enhance the luminol ECL intensity.

3.6. Application of the immunosensor

To monitor the feasibility of the developed immunosensor, recovery experiments were performed by standard addition methods in human serum. The results were shown in Table 1 and the recovery was in the range of 98.6–109.8%, which demonstrated that our strategy could be considered as an optional scheme for detection of IgG in clinical diagnostics.

4. Conclusion

In summary, we have developed a simple and highly sensitive luminol ECL immunosensor by combining the amplification capability of HCR with the enzymatic catalysis to produce co-reactant in situ. Here, due to HCR, massive GOD was attached on the sensing surface and exhibited efficient catalysis towards glucose to in situ generate H_2O_2, which significantly enhanced the ECL response of luminol and further improved the sensitivity of the immunosensor. The proposed immunosensor showed high sensitivity, wide linear range, satisfying stability, acceptable precision and reproducibility. Thus, this strategy could be extended to the detection of other proteins.

Acknowledgments

This work was financially supported by the NNSF of China (21275119 and 21075100), Ministry of Education of China (Project 708073), Natural Science Foundation of Chongqing City (CSTC-2009BA1003 and CSTC-2011BA7003), Specialized Research Fund for the Doctoral Program of Higher Education (20100182110015) and the Postgraduate Science and Technology Innovation Program of Southwest China University (Grant no. XDJK2012A004 and XDJK2013A008).

Appendix A. Supporting information

Supplementary data associated with this article can be found in the online version at http://dx.doi.org/10.1016/j.talanta.2013.06.027.

References

[1] M.M. Richter, Chem. Rev. 104 (2004) 3003–3036.
[2] W.J. Miao, Chem. Rev. 108 (2008) 2506–2553.
[3] P. Bertoncello, R.J. Forster, Biosens. Bioelectron. 24 (2009) 3191–3200.
[4] S.J. Xu, Y. Liu, T.H. Wang, J.H. Li, Anal. Chem. 83 (2011) 3817–3823.
[5] Y.F. Cheng, R. Yuan, Y.Q. Chai, H. Niu, Y.L. Cao, H.J. Liu, L.J. Bai, Y.L. Yuan, Anal. Chim. Acta 745 (2012) 137–142.
[6] X. Cai, J.L. Yan, H.H. Chu, M.S. Wu, Y.F. Tu, Sensor. Actuat. B Chem. 143 (2010) 655–659.
[7] S.R. Yuan, R. Yuan, Y.Q. Chai, L. Mao, X. Yang, Y.L. Yuan, H. Niu, Talanta 82 (2010) 1468–1471.
[8] H.L. Qi, C. Wang, X.Y. Qiu, Q Gao, C.X. Zhang, Talanta 100 (2012) 162–167.
[9] H. Niu, R. Yuan, Y.Q. Chai, L. Mao, H.J. Liu, Y.L. Cao, Biosens. Bioelectron. 39 (2013) 296–299.
[10] H.J. Wang, R. Yuan, Y.Q. Chai, H. Niu, Y.L. Cao, H.J. Liu, Biosens. Bioelectron. 37 (2012) 6–10.
[11] G.F. Jie, P. Liu, S.S. Zhang, Chem. Commun. 46 (2010) 1323–1325.
[12] Z.H. Guo, T.T. Hao, J. Duan, S. Wang, D.Y. Wei, Talanta 89 (2012) 27–32.
[13] H. Niu, R. Yuan, Y.Q. Chai, L. Mao, Y.L. Yuan, Y.L. Cao, Y. Zhuo, Chem. Commun. 47 (2011) 8397–8399.
[14] Y.L. Cao, R. Yuan, Y.Q. Chai, L. Mao, H. Niu, H.J Liu, Y. Zhuo, Biosens. Bioelectron. 31 (2012) 305–309.
[15] G.F. Wang, H. Huang, B.J. Wang, X.J Zhang, L. Wang, Chem. Commun. 48 (2012) 720–722.
[16] B. Zhang, B.Q. Liu, D.P. Tang, R.H. Niessner, G.N. Chen, Anal. Chem. 84 (2012) 5392–5399.
[17] J. Xu, J Wu, Ch. Zong, H.X. Ju, F. Yan, Anal. Chem. 85 (2013) 3374–3379.
[18] R.M. Dirks, N.A. Pierce, Proc. Natl., Acad. Sci. U.S.A 101 (2004) 15275–15278.
[19] L.M. Lu, X.B. Zhang, R.M. Kong, B. Yang, W.H. Tan, J. Am. Chem. Soc. 133 (2011) 11686–11691.
[20] J. Huang, Y. Wu, Y. Chen, Z. Zhu, X. Yang, C. Yang, K. Wang, W. Tan, Angew. Chem., Int. Ed. 50 (2011) 401–404.
[21] Q.W. Xue, Z.G. Wang, L. Wang, W. Jiang, Bioconjugate Chem. 23 (2012) 734–739.
[22] J.J. Zhao, C.F. Chen, L.L. Zhang, J.H. Jiang, R.Q. Yu, Biosens. Bioelectron. 36 (2012) 129–134.
[23] Y. Chen, J. Xu, J. Su, Y. Xiang, R Yuan, Y.Q. Chai, Anal. Chem. 84 (2012) 7750–7755.
[24] G. Jie, B. Liu, H. Pan, J.J. Zhu, H.Y. Chen, Anal. Chem. 79 (2007) 5574–5581.
[25] A. Galal, N.F. Atta, E.H. El-Ads, Talanta 93 (2012) 264–273.
[26] W. Wei, X. Tao, C. Hua, Langmuir 24 (2008) 2826–2833.
[27] Y. Liu, D. Yu, C. Zeng, Z. Miao, L. Dai, Langmuir 26 (2010) 6158–6160.
[28] H.F. Chen, D.P. Tang, B. Zhang, B.Q. Liu, Y.L. Cui, G.N. Chen, Talanta 91 (2012) 95–102.
[29] C.F. Chen, J.J. Zhao, J.H. Jiang, R.Q. Yu, Talanta 101 (2012) 357–361.
[30] S. Kochmann, T. Hirsch, O.S. Wolfbeis, Trac-Trends Anal. Chem. 39 (2012) 87–113.
[31] D. Li, M.B. Muller, S. Gilje, R.B. Kaner, G.G Wallace, Nat. Nanotechnol 3 (2008) 101–105.
[32] F. Lopez-Gallego, L. Betancor, A. Hidalgo, N. Alonso, G. Fernandez-Lorente, Jose M. Guisan, R. Fernandez-Lafuente, Enzyme Microb. Technol. 37 (2005) 750–756.
[33] K. Hernandez, R. Fernandez-Lafuente, Enzyme Microb. Technol. 48 (2011) 107–122.
[34] L. Mao, R. Yuan, Y.Q. Chai, Y. Zhuo, W. Jiang, Analyst 136 (2011) 1450–1455.